ELSEVIER

Chemical Physics 220 (1997) 115–124

Chemical Physics

A three-body calculation for collision-induced dissociation

Kazufumi Sakai

Department of Physics, Gakushuin University, Mejiro 1-5-1, Toshima-ku, Tokyo 171, Japan

Received 16 December 1996

Abstract

A formulation of the distorted-wave Born approximation for the dissociative reaction A + BC → A + B + C is obtained using the T-matrix representation. The computational procedures for obtaining the cross section are presented. Numerical values of the $Ar + H_2 \rightarrow Ar + H + H$ reaction are calculated with the analytic potential surface $BC_3(6,8)$ when the total energies of the system are 0.3, 0.5, 1.0 and 1.2 eV. Present results are compared with those of a Monte Carlo trajectory study and the available-energy hard-sphere model. The cross sections of the reaction for the initial diatomic state $v = 4$ and $v = 6$ $j = 0$ are much smaller than those obtained from quasi-classical trajectory (QCT) calculations, but those for the initial state $v = 10$ and $v = 14$ $j = 0$ are close to the cross sections calculated from QCT. We also calculated the rate constants for the initial state $v = 4$ $j = 0$ at six different temperatures. The rate constant of the present calculation at temperature $T = 4500$ K is about a half of that obtained from QCT. © 1997 Published by Elsevier Science B.V.

Keywords: DWBA; Atom–molecular collisions; CID

1. Introduction

Collision-induced dissociation (CID) of molecules is a very interesting reaction at high temperatures or with a weakly bound colliding partner in chemistry. From a theoretical point of view, this process is also interesting and is considered to be a special kind of reaction because the final product consists of three free particles rather than two, as is normally the case in a reaction. There have been many tests of the quasiclassical trajectory method. On the other hand, only three purely quantal calculations have been published: the wave packet approach [1,2], Delves' coordinate method [3], and a Faddeev-AGS calculation [4]. It is difficult to apply close-coupling methods developed for inelastic and reactive scattering to dissociation process because of the presence of the dissociative continuum.

The distorted-wave Born approximation (DWBA) has been developed by some authors in the case of inelastic and reactive scattering [5–7]. The comparison between the results of close coupling methods and those of the DWBA shows that the DWBA is a suitable approximation in some cases (see Ref. [5]). Furthermore, many authors have discussed the dependence of the cross section on the choice of the potential energy surface.

In this paper, we formulated the CID process for atom–molecular collisions using DWBA and calculated the cross sections employing the realistic potential energy surface suggested by Le Roy and Carley [8] for the process $Ar + H_2 \rightarrow Ar + H + H$. Some

PII S0301-0104(97)00092-X

assumptions are required to use the Le Roy and Carley potential surface in CID process because of the restriction of interatomic distance r and relative distance R. This will be discussed in the numerical procedure section.

2. Formulation

Exact solution of atom–molecular scattering problems requires the solution of the complete Schrödinger equation which involves both the electronic and nuclear motion. However, for the thermal energy region, the Born–Oppenheimer approximation is valid to separate the motion of the nuclei and the electrons. Employing this method, we get the Schrödinger equation which depends on the coordinates of nuclei only:

$$(H-E)\Psi(\boldsymbol{R},\boldsymbol{r})=0. \tag{2.1}$$

Here, in the center of mass system,

$$H=-\frac{\hbar^2}{2\mu_1}\nabla_R^2-\frac{\hbar^2}{2\mu_2}\nabla_r^2+V_T(R,r,\theta). \tag{2.2}$$

μ_1 and μ_2 are appropriate reduced masses:

$$\mu_1=\frac{M_A(M_B+M_C)}{M_A+M_B+M_C},$$

$$\mu_2=\frac{M_BM_C}{M_B+M_C} \tag{2.3}$$

with M_A, M_B, M_C the masses of the atoms and $V_T(R,r,\theta)$ the potential energy surface. The scattering geometry is shown in Fig. 1.

The differential cross section for the CID process for the transition from the entrance channel (a) to the exit channel (b), employing the transition matrix (T matrix) approach, is given by

$$\frac{d\sigma_{ba}}{d\Omega_{k_b}}=\frac{\mu_1^2k_b}{(2\pi\hbar^2)^2k_a}|T_{ba}|^2 \tag{2.4}$$

in the center of mass system, where k_a, k_b are the momenta of the incident and the scattered atom. We take the z-axis as the direction of the incident momentum $\boldsymbol{k}_a$, and the angular momentum projections are referred to this axis. The transition matrix T_{ba}, in the prior interaction form, is given by

$$T_{ba}=\langle\chi_b^{(-)}|V_a'|\Psi_a^{(+)}\rangle, \tag{2.5}$$

where $\chi_b^{(-)}$ is the eigenfunction of $H-V_b'$ with energy E satisfying the incoming wave boundary condition, and $\Psi_a^{(+)}$ is the eigenfunction of H with the same energy E satisfying the outgoing boundary conditions. The potentials V_a' and V_b' are defined as

$$V_a'=V_T(R,r,\theta)-V_{AB}(r)-V_a^0(R),$$

$$V_b'=V_T(R,r,\theta)-V_{AB}(r)-V_b^0(R), \tag{2.6}$$

where $V_{AB}(r)=V_T(\infty,r,\theta)$ and $V_a^0(R)$ and $V_b^0(R)$ are the spherically averaged static potentials.

If we substitute for $\Psi_a^{(+)}$ a wave function $\chi_a^{(+)}$ which is an eigenfunction of $H-V_a'$, we have the distorted-wave Born approximation

$$T_{ba}(\mathrm{DWBA})=\langle\chi_b^{(-)}|V_a'|\chi_a^{(+)}\rangle. \tag{2.7}$$

The $\chi_b^{*(-)}$ is then of the form

$$\chi_b^{*(-)}(\boldsymbol{R},\boldsymbol{r})=\chi_{k_b}^{*(-)}(\boldsymbol{R})\eta_b^{*(-)}(\boldsymbol{r}), \tag{2.8}$$

where $\chi_{k_b}^{(-)}$ is the elastically scattered wave function of the receding atom with final momentum k_b and $\eta_b^{(-)}(\boldsymbol{r})$ is the residual dissociated H + H wave function. These functions are given by

$$\chi_{k_b}^{*(-)}(\boldsymbol{R})=4\pi\sum_{\ell'm}(-i)^{\ell'}\exp(i\delta_{\ell'})L_{\ell'}^*(R)Y_{\ell'm}^*(\hat{R})\times Y_{\ell'm}(\hat{k}_b), \tag{2.9}$$

$$\eta_b^{*(-)}(\boldsymbol{r})=\sqrt{\frac{2}{\pi}}\sum_{j'}\sum_{m''}(-i)^{j'}\exp(i\delta_{j'})L_{j'}^*(r)\times Y_{j'm''}^*(\hat{r})Y_{j'm''}(\hat{k}_{j'}), \tag{2.10}$$

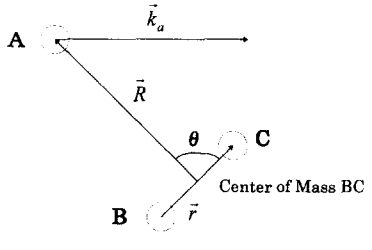

Fig. 1. Geometory of the scattering between an atom and a diatomic molecule.

where $\delta_{\ell'}$, $\delta_{j'}$ are phase shifts: The radial wave functions $L_{\ell'}(r)$ and $L_{j'}(r)$ satisfy the following asymptotic behaviors:

$$L_{\ell'}(R\to\infty)\approx\frac{\sin\left(k_{\mathrm{b}}R-\frac{1}{2}\ell'\pi+\delta_{\ell'}\right)}{k_{\mathrm{b}}R},$$

$$L_{j'}(r\to\infty)\approx\frac{\sin\left(k_{j'}r-\frac{1}{2}j'\pi+\delta_{j'}\right)}{k_{j'}r}. \tag{2.11}$$

The spherical harmonics are defined as follows:

$$Y_{\ell m}(R)=(-1)^{m}\sqrt{\frac{(2\ell+1)(\ell-m)!}{4\pi(\ell+m)!}}\times P_{\ell}^{m}(\cos\theta')\exp(im\phi'), \tag{2.12}$$

where P_{ℓ}^{m} is the associated Legendre polynomial, and θ', ϕ' are the polar angles of $\hat{R}$ with respect to $\hat{z}$. The entrance channel wave function is given by

$$\chi_{\mathrm{a}}^{(+)}(\boldsymbol{R},\boldsymbol{r})=\chi_{k_{\mathrm{a}}}^{(+)}(\boldsymbol{R})\eta_{\mathrm{a}}(\boldsymbol{r}), \tag{2.13}$$

where

$$\chi_{k_{\mathrm{a}}}^{(+)}(R)=\sqrt{4\pi}\sum_{\ell}\sqrt{(2\ell+1)}\,i^{\ell}\exp(i\delta_{\ell})L_{\ell}(R)Y_{\ell 0}(\hat{R}). \tag{2.14}$$

$L_{\ell}(r)$, $\eta_{\mathrm{a}}(\boldsymbol{r})$ are given by

$$L_{\ell}(R\to\infty)\approx\frac{\sin\left(k_{\mathrm{a}}R-\frac{1}{2}\ell\pi+\delta_{\ell}\right)}{k_{\mathrm{a}}R} \tag{2.15}$$

and

$$\eta_{\mathrm{a}}(\boldsymbol{r})=B_{vj}(r)Y_{jm}(\hat{r}). \tag{2.16}$$

The v, j, m are the vibrational, rotational quantum number and the rotational projection of the initial target molecule. We thus obtain entrance and exit channel wave functions as follows:

$$\chi_{\mathrm{a}}^{(+)}(\boldsymbol{R},\boldsymbol{r})=\sqrt{4\pi}\sum_{\ell}\sum_{J}\sqrt{2\ell+1}\,i^{\ell}\exp(i\delta_{\ell})L_{\ell}(R)B_{vj}(r)\times\langle 10jm|Jm\rangle\mathscr{Y}_{\ell j}^{Jm}(\hat{R},\hat{r}) \tag{2.17}$$

and

$$\chi_{\mathrm{b}}^{*(-)}(\boldsymbol{R},\boldsymbol{r})=\sqrt{32\pi}\sum_{\ell'}\sum_{j'm''}\sum_{J}\sum_{m-m''}(-i)^{\ell'+j'}\times\exp\left[i(\delta_{\ell'}+\delta_{j'})\right]\langle\ell' m-m'' j'm''|Jm\rangle\times L_{\ell'}^{*}(R)Y_{\ell' m-m''}(\hat{k}_{\mathrm{b}})Y_{j'm'}(\hat{k}_{j'})\mathscr{Y}_{\ell' j'}^{*Jm}(\hat{R},\hat{r}), \tag{2.18}$$

where

$$\mathscr{Y}_{j_1j_2}^{JM}(\hat{R},\hat{r})=\sum_{m_1m_2}\langle j_1m_1j_2m_2|JM\rangle Y_{j_1m_1}(\hat{R})Y_{j_2m_2}(\hat{r}). \tag{2.19}$$

In Eqs. (2.17) and (2.18), we used the representation in which total angular momentum J is diagonal.

The transition matrix T_{ba} is then given by Eq. (2.7). If we substitute the harmonic expansion of $V_{\mathrm{a}}'(R,r,\theta)$, given by

$$V_{\mathrm{a}}'(R,r,\theta)=\sum_{\ell''}V_{\mathrm{a}}^{\ell''}(R,r)P_{\ell''}(\cos\theta), \tag{2.20}$$

$$V_{\mathrm{a}}^{\ell''}(R,r)=\frac{(2\ell''+1)}{2}\int_{0}^{\pi}P_{\ell''}(\cos\theta)V_{\mathrm{a}}'(R,r,\theta)\sin\theta\,\mathrm{d}\theta \tag{2.21}$$

and carry out several integrations explicitly, we have

$$\begin{aligned}T_{\mathrm{ba}}(\mathrm{DWBA})&=\sqrt{128\pi^2}\sum_{\ell'}\sum_{j'm''}\sum_{J}\sum_{m-m''}\sum_{\ell''}\sum_{\ell}(-1)^{-J-\ell''}\times i^{\ell-\ell'-j'}\exp\left[i(\delta_{\ell}+\delta_{\ell'}+\delta_{j'})\right]\\&\times\frac{(2\ell+1)\sqrt{(2j+1)(2\ell'+1)(2j'+1)}}{2\ell''+1}\times\langle i0i'0|\ell''0\rangle\langle j'0j0|\ell''0\rangle\langle\ell 0jm|Jm\rangle\\&\times\langle\ell' m-m'' j'm''|Jm\rangle\begin{Bmatrix}\ell' & j' & J\\ j & \ell' & \ell''\end{Bmatrix}\times Y_{j'm''}(\hat{k}_{j'})Y_{\ell''m-m''}(\hat{k}_{\mathrm{b}})\\&\times\int\int\mathrm{d}R\,\mathrm{d}r R^2r^2L_{\ell'}^{*}(R)L_{j'}^{*}(r)V_{\mathrm{a}}^{\ell''}(R,r)L_{\ell}(R)\times B_{vj}(r),\end{aligned} \tag{2.22}$$

where

$$\begin{Bmatrix} \ell' & j' & J \\ j & \ell' & \ell'' \end{Bmatrix}$$

is the $6j$ symbol.

The differential cross section is expressed as

$$\frac{\mathrm{d}\sigma_{ba}}{\mathrm{d}\Omega_{k_b}} = \frac{\mu_1^2}{(2\pi\hbar^2)^2}\frac{k_b}{k_a}\frac{1}{2j+1}\sum_m \int \mathrm{d}k_{j'}|T_{ba}|^2 \tag{2.23}$$

in the center of mass system, where we have averaged the initial substates m and integrated over the final substates $\boldsymbol{k}_{j'}$.

The total cross section is given by

$$\sigma_{ba} = \mathrm{d}\Omega_{k_b}\left(\frac{\mathrm{d}\sigma_{ba}}{\mathrm{d}\Omega_{k_b}}\right) = \frac{\mu_1^2}{(2\pi\hbar^2)^2}\frac{k_b}{k_a}\frac{1}{(2j+1)} \times \sum_m \int \mathrm{d}\Omega_{k_b}\int \mathrm{d}\hat{k}_{j_b}|T_{ba}|^2. \tag{2.24}$$

For a given initial total energy E, the energy of the excited continuum state can range from zero to E, or $k_{j'}$ may range from zero to $\sqrt{2\mu_2 E/\hbar^2}$. To obtain the dissociative cross section we sum over these final states. Using Eq. (2.24), the dissociative cross section from a given initial state may be written as,

$$\sigma_{ba}(\mathrm{CID}) = \int_0^{k_{\max}} \sigma_{ba} k_{j'}^2 \,\mathrm{d}k_{j'}, \tag{2.25}$$

where

$$k_{\max} = \sqrt{2\mu_2 E/\hbar^2}. \tag{2.26}$$

The rate constant is defined by

$$\langle v_a \sigma_{ba}(v_a)\rangle = 4\pi N\int_{v_a^{\min}}^{\infty} \sigma_{ba}(v_a) v_a^3 \exp\left(\frac{-\mu_1 v_a^2}{kT}\right)\mathrm{d}v_a, \tag{2.27}$$

where v_a is a velocity of the incoming atom, k is the Boltzmann's constant, and T is the temperature. N is given by

$$N\int \exp\left(\frac{-\mu_1 v_a^2}{2kT}\right)\mathrm{d}\boldsymbol{v}_a = 1, \tag{2.28}$$

and $v_a^{\min}$ is a minimum velocity of the incoming atom for dissociation given by

$$v_a^{\min} = \sqrt{\frac{-2E_B}{\mu_1}}, \tag{2.29}$$

where E_B is the energy of the initial molecule AB. From Eqs. (2.27) and (2.28), we get the rate constant as follows:

$$\langle v_a \sigma_{ba}(v_a)\rangle = \sqrt{\frac{2}{\pi}}\left(\frac{\mu_1}{kT}\right)^{3/2} \times \int_{v_a^{\min}}^{\infty} \sigma_{ba}(v_a) v_a^3 \exp\left(\frac{-\mu_1 v_a^2}{2kT}\right)\mathrm{d}v_a. \tag{2.30}$$

3. Numerical procedures and results

To illustrate the computational aspects of the present method, we present in this section the calculation of the cross sections for the process $Ar + H_2 \rightarrow Ar + H + H$. Employing the Le Roy and Carley potential energy surface $BC_3(6,8)$, we evaluated the partial cross sections for the initial states $v = 4$, $j = 0$, $v = 6$, $j = 0$, $v = 10$, $j = 0$ and $v = 14$, $j = 0$ as a function of total angular momentum. The total energies of the system are chosen to be 0.3, 0.5, 1.0, and 1.2 eV in all calculations. To show our modification of $BC_3(6,8)$, we explain this potential in detail.

The total potential of $Ar + H_2$ system is

$$V_T(R,r,\theta) = V_{AB}(r) + V_3(R,r,\theta), \tag{3.1}$$

where V_{AB} is the interatomic potential of diatomic molecule AB and $V_3(R,r,\theta)$ is the three-body interaction potential $BC_3(6,8)$. We chose the Morse potential as the intramolecular interaction potential whose parameters are given by

$$D_e = 4.7466\,\text{a.u.},\quad \alpha = 1.04435\,\text{a.u.},\quad r_0 = 1.40083\,\text{a.u.} \tag{3.2}$$

The three-body interaction $V_3(R,r,\theta)$ is expanded in the form

$$V_3(R,r,\theta) = \sum_{k=0}^{3}\sum_{n=0,2} h^k P_n(\cos\theta) V_{nk}(R), \tag{3.3}$$

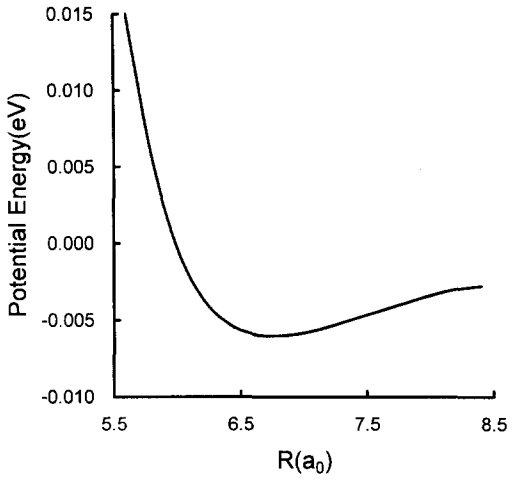

Fig. 2. The spherical average of the $BC_3(6,8)$ potential surface as a function of the distance R at $r = 1.4011$ Å.

where R is the distance between the atom Ar and the H_2 center of mass. h is defined by

$$h = \frac{r - r_0}{r_0}, \tag{3.4}$$

and θ is the angle between $\boldsymbol{R}$ and the axis of the diatomic molecule. The radial strength functions $V_{nk}(R)$ is given by

$$V_{nk}(R) = A^{nk}\exp(-\beta_n R) - D(R)\left(\frac{C_6^{nk}}{R^6} + \frac{C_8^{nk}}{R^8}\right), \tag{3.5}$$

where

$$D(R) = \exp\left[-4(R_0/R - 1)^2\right] \quad \text{for } R < R_0,$$
$$D(R) = 1 \quad \text{for } R > R_0. \tag{3.6}$$

The constants A^{nk}, C^{nk} are defined by

$$A = \left[w(8 - R_e D_1) - \frac{2D_0 C_6}{R_e^6}\right]\frac{\exp(\beta R_e)}{\beta R_e - 8 + R_e D_1} \tag{3.7}$$

and

$$C_8 = \left[\frac{(6 - R_e D_1 - \beta R_e)C_6}{R_e^6} + \frac{w\beta R_e}{D_0}\right] \times \frac{R_e^8}{\beta R_e - 8 + R_e D_1}, \tag{3.8}$$

where $D_0 = D(R = R_e)$ and $D_1 = [\partial D(R)/\partial R]_{R=R_e}$. The parameters are listed in Table V of Ref. [8]. Fig. 2 shows the spherical average of the $BC_3(6,8)$ potential as a functions of the distance R at $r = 1.4011$ a.u. This potential energy surface is restricted to the region of $0 < r < 1.9$ Åand $R > 3.2$ Å. In the case of a CID process, the potential is required to be accurate for large r and R because of the presence of dissociative continuum. We replace the r dependent part of $BC_3(6,8)$ potential as follows:

$$h = (r - r_0)/r_0 \quad \text{for } r < r_0,$$
$$h = (r - r_0)/r \quad \text{for } r > r_0. \tag{3.9}$$

In this way, we prevent the variable h from increasing without bound at large r. Furthermore, in the final state, the short-range distance R affects the final repulsive potential $V_b^0(R)$ and pushes out the final dissociative wave function. It causes the cross section to be very small. Then, we used the $V_3(R = 1.0\text{Å}, r, \theta)$ in the region of small distance $R(R < 1.0\text{Å})$.

The radial wave function $L_\ell(R)$ of the incident and scattered atoms is obtained by solving Schrödinger equations

$$\left\{\frac{d^2}{dR^2} + k^2 - \frac{2\mu V(R)}{\hbar^2} - \frac{\ell(\ell+1)}{R^2}\right\}u_\ell(R) = 0. \tag{3.10}$$

Numerov's method is used with a suitable power series starting from $R = 0$. Here u_ℓ is the unnormalized wave function which has the form

$$u_\ell(R) = A_\ell R\left[j_\ell(kR)\cos\delta_\ell - n_\ell(kR)\sin\delta_\ell\right] \tag{3.11}$$

in the region where $V(R) = 0$. Here j_ℓ and n_ℓ are the spherical Bessel and Neumann function. Using the relation between $u_\ell(R)$ and $L_\ell(R)$,

$$L_\ell(R) = \frac{A_\ell u_\ell(R)}{R}, \tag{3.12}$$

and matching the solutions at R_1 and R_2 in the region where $V(R) = 0$, the factor A_ℓ is given by

$$A_\ell = R_1\frac{j_\ell(kR_1)\cos\delta_\ell - n_\ell(kR_1)\sin\delta_\ell}{u_\ell(R_1)}. \tag{3.13}$$

The phase shift is

$$\tan\delta_\ell = \frac{R_1 j_\ell(kR_1)u_\ell(R_2) - R_2 j_\ell(kR_2)u_\ell(R_1)}{R_1 n_\ell(kR_1)u_\ell(R_2) - R_2 n_\ell(kR_2)u_\ell(R_1)}. \tag{3.14}$$

In Eqs. (3.13) and (3.14), R_1 and R_2 are chosen to be $R_1 - R_2 = 0.9$ a.u. The numerical accuracies are not sensitive to the choices of the two points.

Using the following equations:

$$\exp(i\boldsymbol{k}\cdot\boldsymbol{R}) = 4\pi\sum i^\ell \exp(i\delta_\ell) L_\ell(R) Y_{\ell m}(\hat{R}) Y^*_{\ell m}(\hat{k}) \tag{3.15}$$

and

$$\langle \exp(i\boldsymbol{k}'\cdot\boldsymbol{R}) | \exp(i\boldsymbol{k}\cdot\boldsymbol{R})\rangle = (2\pi)^3\delta(\boldsymbol{k}-\boldsymbol{k}'), \tag{3.16}$$

we get

$$N^2 = \frac{1}{(2\pi)^3}. \tag{3.17}$$

The normalization factor of the continuum wavefunction is determined by following equation:

$$\sum_{\ell m}\sum_{\ell' m'} N^2 \int (4\pi)^2 L_\ell(r) Y_{\ell m}(\hat{r}) Y^*_{\ell m}(\hat{k}) L_{\ell'}(r) \times Y^*_{\ell' m'}(\hat{r}) Y_{\ell' m'}(\hat{k}')\, \mathrm{d}r^3 = \delta(\boldsymbol{k}-\boldsymbol{k}'). \tag{3.18}$$

To solve the molecular wave functions, we use the same approximate treatment whose detailed explanation is described elsewhere [9]. The molecular wave function is shown in Fig. 3.

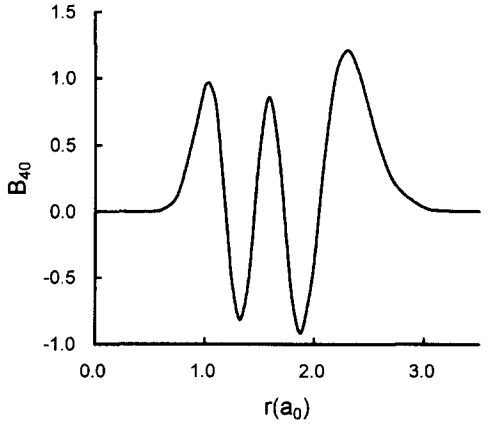

Fig. 3. Molecular wave function for $v = 4$ $j = 0$ as a function of intermolecular distance r.

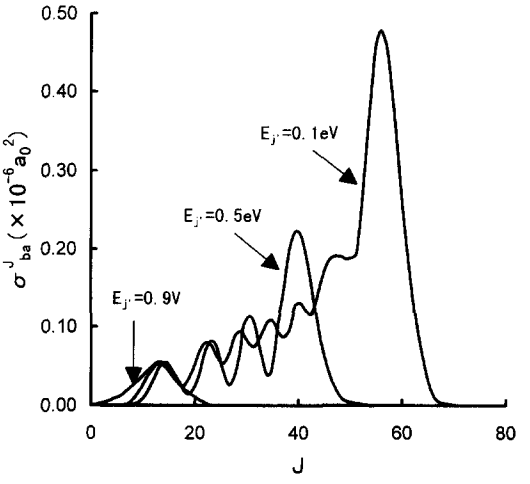

Fig. 4. Partial cross sections as a function of J for initial diatomic state $v = 4$ $j = 0$.

In the present calculation, the maximum value of J was chosen to be 200 at all energies. This is sufficient for obtaining converged cross sections. Some partial cross sections as function of the total

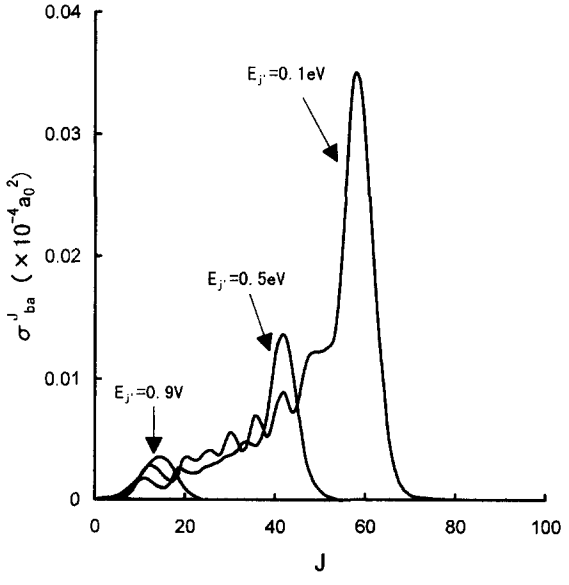

Fig. 5. Partial cross sections as a function of J for initial diatomic state $v = 6$ $j = 0$.

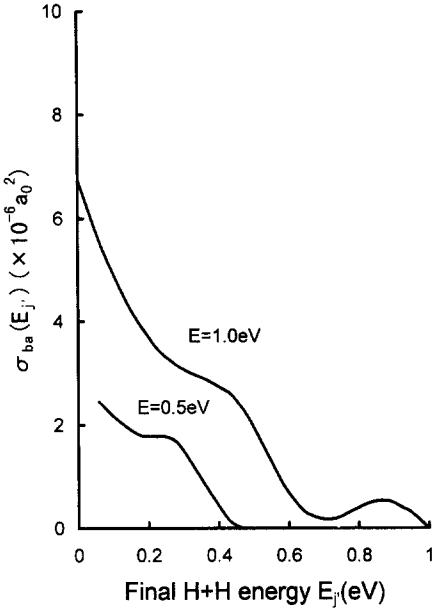

Fig. 6. Cross sections for initial diatomic state $v=4$ $j=0$ as a function of final H+H energy $E_{j'}$.

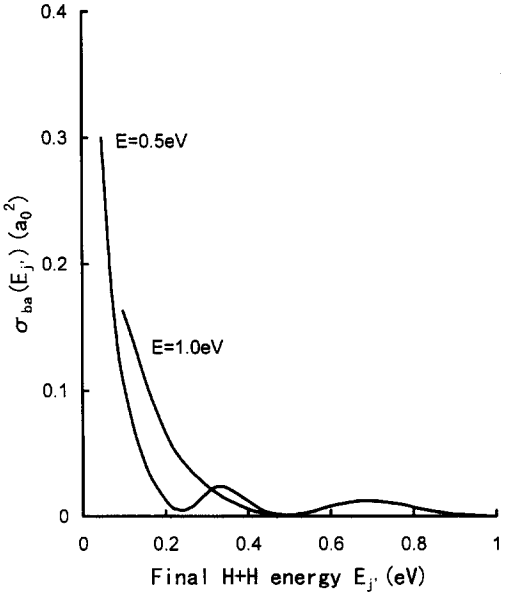

Fig. 8. Cross sections for initial diatomic state $v=10$ $j=0$ as a function of final H+H energy $E_{j'}$.

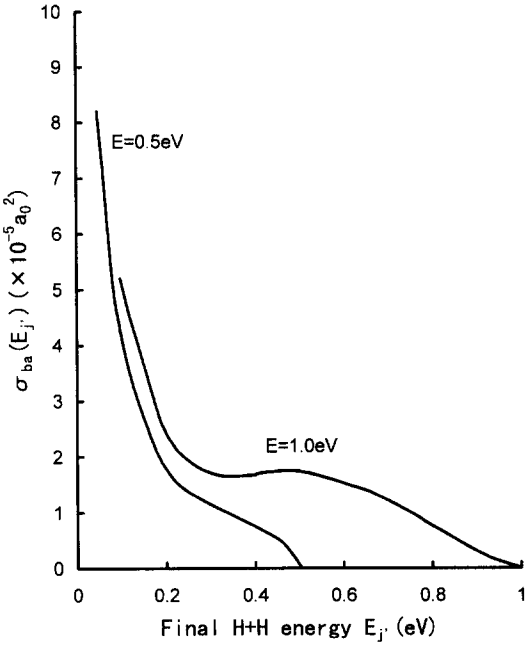

Fig. 7. Cross sections for initial diatomic state $v=6$ $j=0$ as a function of final H+H energy $E_{j'}$.

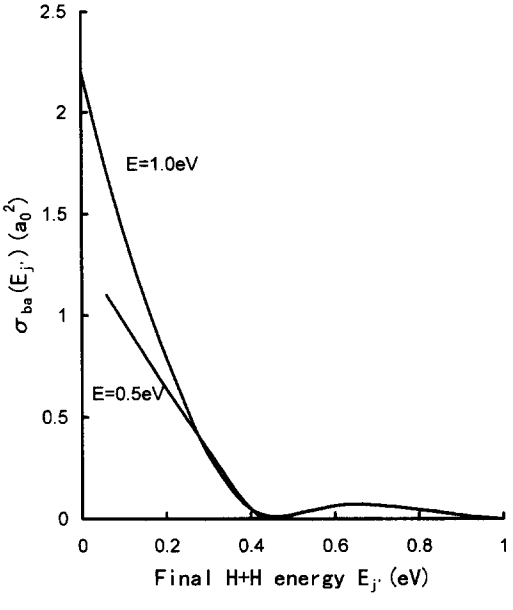

Fig. 9. Cross sections for initial diatomic state $v=14$ $j=0$ as a function of final H+H energy $E_{j'}$.

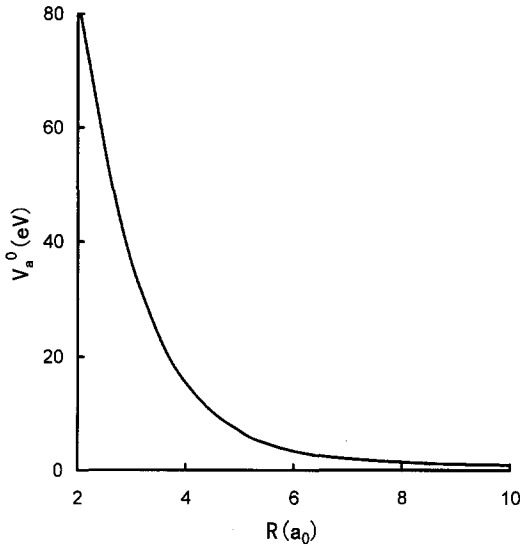

Fig. 10. Spherically averaged static potential for the initial diatomic state $v = 4$ $j = 0$.

angular momentum quantum number J are shown in Figs. 4 and 5. Figs. 6–9 show the cross sections as a function of final H + H energy with total energy 1 and 0.5 eV.

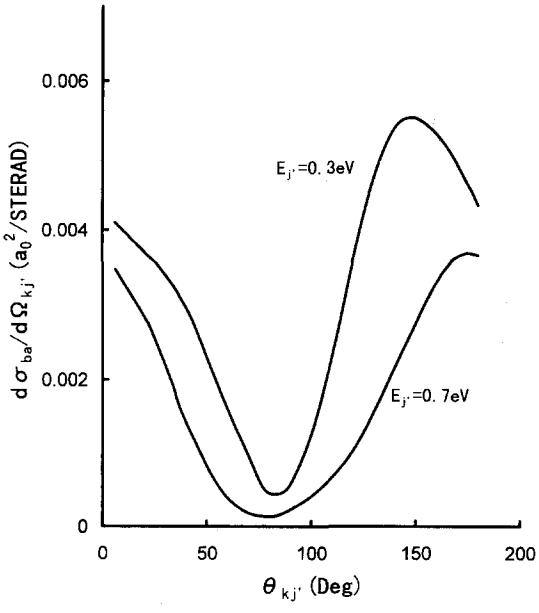

Fig. 11. The differential cross sections as a function of the angle of the residual dissociated H + H.

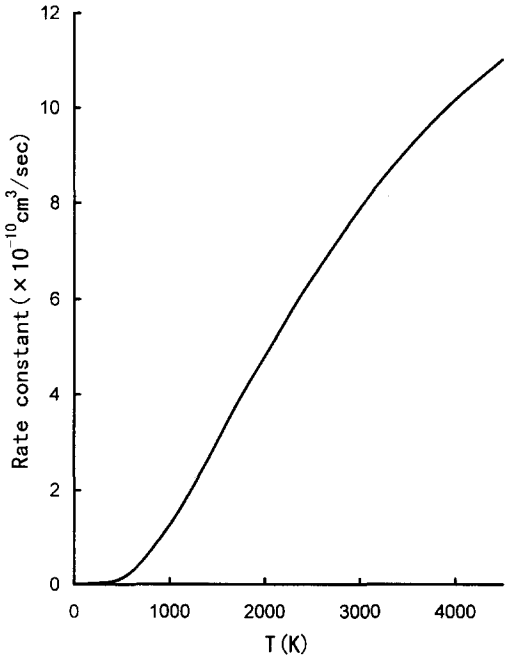

Fig. 12. The rate constant for initial diatomic state $v = 14$ $j = 0$ as a function of the temperature T(K).

To reduce the computer time, we used the prior form of T-matrix which is

$$T_{ba}(\mathrm{DWBA}) = \langle \chi_b^{(-)} | V_a' | \chi_a^{(+)} \rangle, \tag{3.19}$$

where

$$V_a'(R,r) = V_T(R,r,\theta) - V_{AB}(r) - V_a^0(R). \tag{3.20}$$

Fig. 10 shows the spherically averaged static potential $V_a^0(R)$ for the initial diatomic state $v = 4$, $j = 0$.

The differential cross section as a function of the angle of the residual dissociated H + H is shown in Fig. 11.

Using Eq. (2.30), we calculated initial state $v = 14$, $j = 0$. The results are shown in Fig. 12.

All programs used in this paper are checked for the case of rotational excitation for $(v,j) = (0,0) \rightarrow (0,2)$ at $E = 0.15$ and 0.25 eV. Our results are compared to those of Choi's [5] and the values and shapes of partial cross section as a function of total angular momentum J are in excellent agreement. This gives us a high level of confidence in the present numerical integration routines.

4. Comparison with other calculations and discussions

The difference between the inelastic collision and CID processes, from the point of view of quantum mechanical DWBA treatment, results only from the final state. If we calculate the final repulsive potential carelessly, the wave function of the scattered atom is pushed outside of the main overlapping region with incoming atomic wave function. It causes the calculated cross section to be very small. It is necessary to calculate this potential in a very large region and to bound the three-body interaction potential. From this point of view, the Le Roy and Carley potential energy surface is not adequate for calculating the CID process because of its limited region of validity. Thus, we need to modify this potential energy surface.

It is interesting to compare our results to a previous Monte Carlo trajectory study [10–12] and the popular available-energy hard-sphere model [13]. The resulting cross sections are given in Table 1. The values of available-energy hard-sphere model were calculated by Blais and Truhlar in their paper [10–12]. We see that the values of hard-sphere model are too large. This model clearly leads to very serious errors especially for the lower-lying states (see Ref. [10]). It is more interesting to compare our results to those of QCT. Table 1 shows that the cross sections of DWBA for upper-lying states are closer to those by QCT than those for lower-lying states. From this, we can predict that the contribution of higher-order scattering process are not negligible for dissociation of $Ar + H_2$. To estimate the cross sections for those states we must use other formulations which involve the higher-order scattering processes such as Coupled Channel DWBA [14] methods.

Another considerable difference between the QCT calculation and the present method is due to the way that the initial bound energies of H_2 are approximated. Blais and Truhlar used the values from ab initio electronic structure calculations. The ab initio results are accurate for internuclear distances less than or equal to 10 a_0. On the other hand, the Morse potential, which we used in this paper, is accurate only for lower-lying states. This difference causes the initial bound energies used here to be much smaller than those used by Blais and Truhlar (see Tables 2 and 3). We can predict that the cross sections for initial bound states $v = 10$ and $v = 14$

Table 1
Total cross sections [a] (a_0^2) for $Ar+H_2$ dissociative collisions with total energies of 0.3 (top entry), 0.5 (second entry), 1.0 (third entry) and 1.2 eV (bottom entry)

	Present (DWBA)	QCT [b]	Hard-sphere model [b]
$v=4\ j=0$	0.919(−4)	–	–
	2.02(−4)	–	–
	3.91(−4)	0.021	38.61
	5.22(−4)	–	–
$v=6\ j=0$	0.697(−4)	–	–
	1.25(−3)	–	–
	2.75(−3)	0.291	48.93
	3.33(−3)	–	–
$v=10\ j=0$	2.04	–	–
	3.00	–	–
	4.37	7.37	85.84
	5.00	–	–
$v=14\ j=0$	60.2	–	–
	85.7	–	–
	63.2	104.63 [c]	–
	60.1	–	–

[a] Multiplicative powers of 10 are given in parentheses.
[b] Reported in Ref. [10].
[c] Reported in Ref. [12].

Table 2
Rate constants [a] for dissociation for initial diatomic state $v = 14$ $j = 0$

Temperature (K)	Rate constants (cm^3/s)	
	Present (DWBA)	QCT [b]
300	2.12(−12)	–
1000	1.30(−10)	–
2000	4.88(−10)	–
3000	7.94(−10)	–
4000	1.02(−9)	–
4500	1.10(−9)	2.1(−9)

[a] Multiplicative powers of 10 are given in parentheses.
[b] Reported in Ref. [12].

Table 3
Comparison of bound energies(eV) of H_2

	Morse potential	ab initio [a]
$v=4,\ j=0$	−2.5831	−2.5862
$v=6,\ j=0$	−1.8283	−1.8105
$v=10,\ j=0$	−0.7116	−0.6147
$v=14,\ j=0$	−0.1125	−0.0173

[a] Reported in Refs. [10,15].

are bigger than present results if we use the ab initio calculation for initial bound states.

It is important that we estimate the accuracy of the DWBA approximation. From Eqs. (2.5) and (2.7), we see that if V_a^0 is close to $V_{T'}$ DWBA is a suitable approximation. However, it is not a simple task to compute the corresponding scattering wave function $\chi^{(\pm)}$. Many calculations and more detailed study of this method are required to predict the accuracy as well as to improve this approximation. Furthermore, for a rigorous description of the dynamics of a collision, it is necessary to use quantum mechanics. From this point of view, DWBA as well as other exact quantum mechanical methods may play important role to elucidate the dynamics of atom–molecule collision. It is not yet possible to compare our results with other quantum mechanical methods. Only further calculations can determine the accuracy of DWBA for CID process.

5. Conclusion

We formulated the collision-induced dissociation process for atom–molecule collisions using the distorted-wave Born approximation and calculated the cross sections employing the realistic potential energy surface suggested by Le Roy and Carley for the process $Ar + H_2 \rightarrow Ar + H + H$. The result is compared with that of the available-energy hard-sphere model and with QCT calculations. We see that the contribution of higher-order scattering processes are not negligible for the process, and if the spherically averaged static potential is close to the total potential of the system, the distorted-wave Born approximation is a suitable approximation.

References

[1] K.C. Kulander, J. Chem. Phys. 69 (1978) 5064.
[2] J.C. Gray, G.A. Fraser, D.G. Truhlar, K.C. Kulander, J. Chem. Phys. Lett. 73 (1980) 5726.
[3] J. Manz, J. Romelt, Chem. Phys. Lett. 77 (1981) 72.
[4] M.I. Halftel, T.K. Lim, Chem. Phys. Lett. 78 (1981) 546.
[5] B.H. Choi, K.T. Tang, J. Chem. Phys. 63 (1975) 1783.
[6] K.T. Tang, M. Karplus, Phys. Rev. A 4 (1971) 1844.
[7] B.H. Choi, K.T. Tang, J. Chem. Phys. 61 (1974) 5147.
[8] R.J. Le Roy, J.C. Carley, Adv. Chem. Phys. 42 (1980) 353.
[9] F. Hermann and S. Skillman, in: Atomic structure calculations (Prentice-Hall, Englewood Cliffs, NJ, 1963) and modified by B.H. Choi for molecular problem.
[10] N.C. Blais, D.G. Truhlar, J. Chem. Phys. 65 (1976) 5335.
[11] N.C. Blais and D.G. Truhlar, in: Potential energy surfaces and dynamics calculations, ed. D.G. Truhlar (Plenum, New York, 1981) p. 431.
[12] N.C. Blais, D.G. Truhlar, J. Chem. Phys. 78 (1983) 2388.
[13] R.H. Fowler and E.A. Guggenheim, in: Statistical thermodynamics (Cambridge Univ. Press, Cambridge 1939) pp. 491–499.
[14] P. Halvick, M. Zhao, D.G. Truhlar, D.W. Schwenke, D.J. Kouri, J. Chem. Soc. Faraday Trans. 86 (1990) 1705.
[15] N.C. Blais, D.G. Truhlar, J. Chem. Phys. 66 (1977) 722.